V European Conference on Computational Fluid Dynamics
ECCOMAS CFD 2010
J. C. F. Pereira and A. Sequeira (Eds)
Lisbon, Portugal,14-17 June 2010

EXTENDED VARIATIONAL MULTISCALE METHODS FOR TURBULENT VARIABLE-DENSITY FLOW AT LOW MACH NUMBER AND PREMIXED COMBUSTION

Volker Gravemeier[*,†], Florian Henke[*,†] and Wolfgang A. Wall[†]

[*]Emmy Noether Research Group "Computat. Multiscale Methods for Turbulent Combustion",
Technische Universität München, Boltzmannstr. 15, D-85747 Garching, Germany,
e-mail: {vgravem,henke}@lnm.mw.tum.de
[†]Institute for Computational Mechanics,
Technische Universität München, Boltzmannstr. 15, D-85747 Garching, Germany,
e-mail: wall@lnm.mw.tum.de

Key words: turbulent variable-density flow, premixed combustion, large-eddy simulation, variational multiscale method, algebraic multigrid, extended finite element method

Abstract. *Problems of combustion are usually mathematically described by a variable-density formulation of the Navier-Stokes equations at low Mach number. Finite volume and finite difference methods have been proposed for large-eddy simulation (LES) of variable-density turbulent flows at low Mach number. Finite element methods, which are often better suited for problems in complex geometries, have so far only been applied to laminar flows of this kind, to the best of our knowledge. We recently proposed an Algebraic Variational Multiscale-Multigrid Method (*AVM^3*) within a finite element framework for LES of turbulent variable-density flow at low Mach number.*

The G-function approach to turbulent premixed combustion problems is based on the flamelet concept. Within this concept, the flame front is modeled as a sharp embedded interface represented by the iso-surface of a level-set function. Because properties of burnt and unburnt gases vary significantly across the interface, the flow field renders discontinuous. To account for jumps in the velocity and the pressure field, an eXtended Finite Element Method (XFEM) is applied. Following this idea, we were able to achieve very promising results for laminar premixed combustions problems. Our efforts towards developing extended variational multiscale methods for turbulent premixed combustion will be presented in this talk.

1 INTRODUCTION

Large-eddy simulation (LES) has successfully been applied to both incompressible (see, e.g., [1]) and compressible (see, e.g., [2]) turbulent flow. More rarely, applications of LES to turbulent variable-density flow at low Mach number are encountered in literature. This is despite the importance of the problems mathematically described by this set of equations. In particular, problems of combustion are usually mathematically described by a variable-density formulation of the Navier-Stokes equations for low-speed flows; see, e.g., [3, 4]. Methods for LES of reactive and/or non-reactive turbulent low-Mach-number flow are proposed, for instance, based on finite-volume approaches in [5, 6, 7] and based on a finite-difference approach in [8]. Finite element methods (FEMs) for non-reactive low-Mach-number flow are described, e.g., in [9, 10, 11] and for reactive flow, e.g., in [12, 13, 14]. However, all aforementioned publications merely addressed *laminar* low-Mach-number flow situations. In particular, to the best of our knowledge, there have not yet been published any studies on FEMs for (non-reactive) variable-density *turbulent* flows at low Mach number.

The framework of an algebraic variational multiscale-multigrid method (AVM^3) was originally proposed in [15] and applied to convection-dominated convection-diffusion problems. It was further developed and extended for application to turbulent incompressible flow in the form of LES in [16]. The AVM^3 is theoretically based on the concept of the variational multiscale approach to LES (VMLES) as originally proposed in [17] and later addressed in [18]; see, e.g., [19] for a review and several references therein. The scale separation underlying the AVM^3 is based on level-transfer operators arising in plain aggregation algebraic multigrid (PA-AMG); see, e.g., [20]. In [21], the AVM^3 was proposed for LES of turbulent variable-density flow at low Mach number. Here, a brief presentation of the AVM^3 for LES of such flow problems will be provided. For elaboration, the reader is referred to [21].

The G-equation approach to turbulent premixed combustion is based on the flamelet concept. Often, chemical length scales can be considered small compared to turbulent length scales. Therefore, a turbulent flame can be modeled as an ensemble of stretched laminar flamelets which are thin reactive-diffusive layers embedded in a non-reacting flow field, see, e.g., [22, 4]. Since the reaction zone can be considered thin in the aforementioned regimes, the flame can be collapsed to a two-dimensional flame front embedded in a three-dimensional discontinuous flow field. The interface is represented by the G-function, which is essentially a level-set function for the scalar G describing the propagation of the flame front. Level-set methods for propagating fronts were first presented in [23]. The position of the flame front is represented by an iso-surface of the level-set function. The G-equation takes into account both the convection velocity of the flow field and the burning velocity at the interface for describing the propagating flame front. Its physical meaning, however, is confined to the flame front itself. An early G-function approach to LES was proposed, e.g., in [24].

EXtended Finite Element Methods (XFEM) are able to represent discontinuities by enriching the finite element function spaces with discontinuous shape functions. This method was originally developed in the context of crack propagation in solid mechanics (see, e.g., [25]) and later extended to a variety of different applications, including two-phase flow problems [26], for example. Large gradients of velocity, pressure, temperature, species mass fraction and material properties are found within the thin reaction zone of a flame. Using the XFEM, the flow field is assumed discontinuous at the flame front, and jumps in velocity and pressure are taken into account via discontinuous enrichment functions. We already achieved very promising results applying an XFEM to the G-equation approach in [27], and the reader is referred to that study for elaboration.

2 GOVERNING EQUATIONS

2.1 Variable-density formulation at low Mach number

Conservation equations for mass, momentum and energy in the domain Ω are given as

$$\frac{\partial \rho}{\partial t} + \nabla \cdot (\rho \mathbf{u}) = 0, \tag{1}$$

$$\rho \frac{\partial \mathbf{u}}{\partial t} + \rho \mathbf{u} \cdot \nabla \mathbf{u} + \nabla p_{\mathrm{hyd}} - \nabla \cdot \left(2\mu \varepsilon' (\mathbf{u})\right) = \rho \mathbf{g}, \tag{2}$$

$$\rho \frac{\partial T}{\partial t} + \rho \mathbf{u} \cdot \nabla T - \nabla \cdot \left(\frac{\lambda}{c_p} \nabla T\right) = \frac{1}{c_p} \left[\frac{dp_{\mathrm{the}}}{dt} + Q\right], \tag{3}$$

where ρ denotes the density, $\mathbf{u}$ the velocity, p_{hyd} the hydrodynamic pressure, μ the viscosity, $\varepsilon' (\mathbf{u}) = \varepsilon (\mathbf{u}) - \frac{1}{3} (\nabla \cdot \mathbf{u}) \mathbf{I}$, with the rate-of-deformation tensor $\varepsilon (\mathbf{u}) = \frac{1}{2} \left(\nabla \mathbf{u} + \left(\nabla \mathbf{u}^{\mathrm{T}}\right)\right)$, $\mathbf{I}$ the identity tensor, $\mathbf{g}$ the gravity force vector, T the temperature, c_p the specific heat capacity at constant pressure (assumed constant), λ the thermal conductivity, p_{the} the thermodynamic pressure and Q a potential heat source. Properties μ and λ are assumed to vary with T according to Sutherland's law:

$$\mu = \left(\frac{T}{T_{\mathrm{ref}}}\right)^{\frac{3}{2}} \left(\frac{T_{\mathrm{ref}} + S}{T + S}\right) \mu_{\mathrm{ref}}, \quad \lambda = \frac{c_p}{\mathrm{Pr}} \mu, \tag{4}$$

using a reference temperature T_{ref}, a reference viscosity μ_{ref}, the Sutherland temperature S, and the Prandtl number $\mathrm{Pr} = \frac{c_p \mu}{\lambda}$. Note that energy conservation (3) is expressed in terms of temperature. Additionally, the equation of state for an ideal gas,

$$\rho = \frac{p_{\mathrm{the}}}{RT}, \tag{5}$$

is assumed based on the gas constant R. Using (5), the mass-conservation equation (1) may be reformulated as

$$\nabla \cdot \mathbf{u} = \frac{1}{T} \left(\frac{\partial T}{\partial t} + \mathbf{u} \cdot \nabla T\right) - \frac{1}{p_{\mathrm{the}}} \frac{dp_{\mathrm{the}}}{dt}. \tag{6}$$

Appropriate initial and boundary conditions need to be defined for the presented system of equations. The configuration of the backward-facing step, which is used as a numerical example below, represents an open system due to the Neumann outflow boundary, which determines the (constant) thermodynamic pressure in this case. In the following, it will already be accounted for the fact that the thermodynamic pressure is constant and that $Q = 0$.

2.2 G-equation approach to premixed combustion

The domain of a premixed combustion problem $\Omega \subset \mathbb{R}^3$ consists of the subdomains Ω^u and Ω^b, denoting the unburnt and the burnt portions of the domain, respectively. They are separated by the interface $\Gamma = \partial\Omega^u \cap \partial\Omega^b$, that is, the flame front. By definition, the normal $\mathbf{n}$ at the interface points towards the unburnt domain.

The total flame speed $\mathbf{v}_\mathrm{f}$ acts on the G-function as a convective velocity for the level-set equation

$$\frac{\partial G}{\partial t} + \mathbf{v}_f \cdot \nabla G = 0. \tag{7}$$

It depends on the convection velocity of the unburnt flow phase $\mathbf{u}^u$ at the flame front and the burning velocity s_L of the flame, which acts in the normal direction to the flame front:

$$\mathbf{v}_\mathrm{f} = \mathbf{u}^u + s_\mathrm{L} \cdot \mathbf{n}. \tag{8}$$

For a planar laminar flame, the burning velocity s_L^0 characterizes a specific chemical reaction. Compared to s_L^0, s_L takes the effects of curvature ($\kappa = \nabla \cdot \mathbf{n}$) and strain into account. The G-equation

$$\frac{\partial G}{\partial t} + \mathbf{u}^u \cdot \nabla G = s_\mathrm{L} |\nabla G| \tag{9}$$

with the normal vector

$$\mathbf{n} = -\frac{\nabla G}{|\nabla G|} \tag{10}$$

defines the shape and position of the flame front Γ implicitly. It is represented by the iso-surface $G_0 = 0$ according to

$$G(\mathbf{x}, t) \begin{cases} > 0 & \forall \mathbf{x} \in \Omega^b \\ = 0 & \forall \mathbf{x} \in \Gamma \\ < 0 & \forall \mathbf{x} \in \Omega^u. \end{cases} \tag{11}$$

The G-function is continuous at the interface and initialized as a *signed distance function* ($|\nabla G(\mathbf{x}, t = 0)|$=1). Problems concerning mass conservation of level set methods are

well known in literature. Reinitialization of the G-function is neccessary, since it looses its signed-distance property during the simulation. The reader is referred to [28] and references therein for a detailed description of various reinitialization techniques. Here, $G(\mathbf{x},t)$ is reinitialized directly by calculating the distance from each grid point to the discrete representation of interface Γ.

The conservation equations for mass and momentum are given by equations (1) and (2) (with $\nabla \cdot \mathbf{u} = 0$, if incompressible flow is assumed), respectively. Each of them hold in the burnt and unburnt domains, with corresponding densities ρ and viscosities μ given as

$$\rho\left(\mathbf{x},t\right) = \begin{cases} \rho^b & \forall \mathbf{x} \in \Omega^b \\ \rho^u & \forall \mathbf{x} \in \Omega^u, \end{cases} \qquad \mu\left(\mathbf{x},t\right) = \begin{cases} \mu^b & \forall \mathbf{x} \in \Omega^b \\ \mu^u & \forall \mathbf{x} \in \Omega^u. \end{cases} \tag{12}$$

The discontinuous flow field interacts with the G-equation in form of a coupled two-field problem.

3 ALGEBRAIC VARIATIONAL MULTISCALE-MULTIGRID METHOD

The key ingredient of the AVM^3 is a small-scale subgrid-viscosity term. For introducing this term, the resolved part of the velocity, $\mathbf{u}^h$, is further decomposed into a large resolved and a small resolved part, besides the unresolved part $\hat{\mathbf{u}}$:

$$\mathbf{u} = \underbrace{\mathbf{u}^{3h} + \delta\mathbf{u}^h}_{\mathbf{u}^h} + \hat{\mathbf{u}}. \tag{13}$$

The space of large resolved velocity scales is identified by a grid of characteristic element length $3h$, whereas the full resolution limit is h. The actual implementation used here performs this separation in a purely algebraic way without need for generating additional grid levels besides the basic one, though. In fact, plain aggregation algebraic multigrid (PA-AMG) is used for generating prolongation and restriction (i.e., level-transfer) operator matrices based on algebraic principles. The respective procedure is not described in detail here. The reader is referred to our earlier publications such as [15] for elaboration.

The small-scale subgrid-viscosity term is based on the physical reasoning that energy transport in turbulent flow mainly occurs between scales of similar size. The present model should particularly account for the effect of unresolved scales on the small resolved scales. The small-scale subgrid viscosity, $\mu_{\mathrm{T}}^{\delta h}$, is also assumed to only depend on the small resolved scales. It is defined by a modified (constant-coefficient) Smagorinsky model as

$$\mu_{\mathrm{T}}^{\delta h} = \rho^h \left(C_{\mathrm{S}} h\right)^2 \left|\varepsilon(\delta\mathbf{u}^h)\right|, \tag{14}$$

with C_{S} denoting the Smagorinsky constant and $\left|\varepsilon(\delta\mathbf{u}^h)\right| = \sqrt{2\varepsilon(\delta\mathbf{u}^h) : \varepsilon(\delta\mathbf{u}^h)}$ the norm of the rate-of-deformation tensor based on the small-scale velocity. The Smagorinsky constant C_{S} is chosen to be 0.1, and no parameter tuning is performed to keep the modeling as simple as possible.

The small-scale subgrid-viscosity term is introduced into a residual-based variational multiscale FE formulation:

$$\left(q^h, \nabla \cdot \mathbf{u}^h\right) + \left(\nabla q^h, \tau_{\mathrm{M}} \mathcal{R}_{\mathrm{M}}^h\right) = \left(q^h, \frac{1}{T^h}\left(\frac{\partial T^h}{\partial t} + \mathbf{u}^h \cdot \nabla T^h\right)\right) \; \forall \, q^h \in \mathcal{V}_p^h, \tag{15}$$

$$\begin{aligned} &\left(\mathbf{v}^h, \rho^h \frac{\partial \mathbf{u}^h}{\partial t}\right) + \left(\mathbf{v}^h, \rho^h \mathbf{u}^h \cdot \nabla \mathbf{u}^h\right) - \left(\nabla \cdot \mathbf{v}^h, p_{\mathrm{hyd}}^h\right) \\ &+ \left(\varepsilon\left(\mathbf{v}^h\right), 2\mu^h \varepsilon'\left(\mathbf{u}^h\right)\right) + \left(\nabla \cdot \mathbf{v}^h, \tau_{\mathrm{C}} \mathcal{R}_{\mathrm{C}}^h\right) + \left(\varepsilon\left(\delta \mathbf{v}^h\right), 2\mu_{\mathrm{T}}^{\delta h} \varepsilon'\left(\delta \mathbf{u}^h\right)\right) \\ &+ \left(\rho^h \mathbf{u}^h \cdot \nabla \mathbf{v}^h, \tau_{\mathrm{M}} \mathcal{R}_{\mathrm{M}}^h\right) - \left(\mathbf{v}^h, \rho^h \tau_{\mathrm{M}} \mathcal{R}_{\mathrm{M}}^h \cdot \nabla \mathbf{u}^h\right) - \left(\rho^h \tau_{\mathrm{M}} \mathcal{R}_{\mathrm{M}}^h \cdot \nabla \mathbf{v}^h, \tau_{\mathrm{M}} \mathcal{R}_{\mathrm{M}}^h\right) \\ &= \left(\mathbf{v}^h, \rho^h \mathbf{g}\right) \; \forall \, \mathbf{v}^h \in \mathcal{V}_{\mathbf{u}}^h, \end{aligned} \tag{16}$$

$$\begin{aligned} &\left(w^h, \rho^h \frac{\partial T^h}{\partial t}\right) + \left(w^h, \rho^h \mathbf{u}^h \cdot \nabla T^h\right) + \left(\nabla w^h, \frac{\lambda^h}{c_p} \nabla T^h\right) + \left(\rho^h \mathbf{u}^h \cdot \nabla w^h, \tau_{\mathrm{E}} \mathcal{R}_{\mathrm{E}}^h\right) \\ &= 0 \; \forall \, w^h \in \mathcal{V}_T^h, \end{aligned} \tag{17}$$

where the discrete residuals of mass, momentum and energy conservation are given as

$$\mathcal{R}_{\mathrm{C}}^h = \nabla \cdot \mathbf{u}^h - \frac{1}{T^h}\left(\frac{\partial T^h}{\partial t} + \mathbf{u}^h \cdot \nabla T^h\right), \tag{18}$$

$$\mathcal{R}_{\mathrm{M}}^h = \rho^h \frac{\partial \mathbf{u}^h}{\partial t} + \rho^h \mathbf{u}^h \cdot \nabla \mathbf{u}^h + \nabla p_{\mathrm{hyd}}^h - \nabla \cdot \left(2\mu^h \varepsilon'\left(\mathbf{u}^h\right)\right) - \rho^h \mathbf{g}, \tag{19}$$

$$\mathcal{R}_{\mathrm{E}}^h = \rho^h \frac{\partial T^h}{\partial t} + \rho^h \mathbf{u}^h \cdot \nabla T^h - \nabla \cdot \left(\frac{\lambda^h}{c_p} \nabla T^h\right). \tag{20}$$

A Pressure-Stabilizing Petrov-Galerkin (PSPG) term appears in (15), and a grad-div term in (16) (last term on the left-hand side of (15) and second term in the second line of (16), respectively). The last term in the second line of (16) represents the small-scale subgrid-viscosity term. The terms in the third line of (16) are, in this order, a Streamline Upwind Petrov-Galerkin (SUPG), a cross-stress and a Reynolds-stress term, all of them being in convective form. An SUPG term is also added to the energy-conservation equation (4). The full formulation taking into all terms in the momentum equation is denoted by ALLSUP in the numerical example below. Taking into account the small-scale subgrid-viscosity term as well as the SUPG term is named AVSSUP. SCRSUP denotes the inclusion of SUPG, cross- and Reynolds-stress terms, and SUPSUP indicates that only the SUPG term is considered.

The stabilization parameters τ_{M} and τ_{C} are defined for the present variable-density equation system as follows:

$$\tau_{\mathrm{M}} = \frac{1}{\sqrt{\left(\frac{2\rho^h}{\Delta t}\right)^2 + \left(\rho \mathbf{u}\right)^h \cdot \mathbf{G} \left(\rho \mathbf{u}\right)^h + C_{\mathrm{I}} \left(\mu^h\right)^2 \mathbf{G} : \mathbf{G}}}, \tag{21}$$

$$\tau_{\mathrm{C}} = \frac{1}{\tau_{\mathrm{M}} \mathbf{g} \cdot \mathbf{g}}, \tag{22}$$

where

$$G_{ij} = \sum_{k=1}^{3} \frac{\partial \xi_k}{\partial x_i} \frac{\partial \xi_k}{\partial x_j}, \quad g_i = \sum_{j=1}^{3} \frac{\partial \xi_j}{\partial x_i} \tag{23}$$

utilize the coordinate system ξ of the element parent domain. The time-step length of the temporal discretization of the problem formulation is denoted by Δt, and C_{I} is a positive constant independent of the characteristic element length h. Adopting (21) for the energy conservation equation yields

$$\tau_{\mathrm{E}} = \frac{1}{\sqrt{\left(\frac{2\rho^h}{\Delta t}\right)^2 + (\rho\mathbf{u})^h \cdot \mathbf{G}\,(\rho\mathbf{u})^h + C_{\mathrm{I}}\left(\frac{\lambda^h}{c_p}\right)^2 \mathbf{G} : \mathbf{G}}}. \tag{24}$$

4 EXTENDED FORMULATION FOR PREMIXED COMBUSTION

EXtended Finite Element Methods (XFEMs) are able to represent discontinuous fields by enriching the function spaces with appropriate discontinuous functions. In the present context of premixed combustion, a Heaviside function is used to represent jumps in velocity and pressure arising from thermal expansion across the interface:

$$H(\mathbf{x},t) = \begin{cases} -1 & \text{if } G(\mathbf{x},t) \leq 0 \\ 1 & \text{if } G(\mathbf{x},t) > 0. \end{cases} \tag{25}$$

All nodes i of elements intersected by the flame front are enriched by additional degrees of freedom $\mathbf{a}_i$ and b_i besides the standard degrees of freedom $\mathbf{u}_i$ and p_i, respectively:

$$\mathbf{u}^h(\mathbf{x},t) = \sum_i N_i(\mathbf{x}) \left[\mathbf{u}_i(t) + \mathbf{a}_i(t) \left(H\left(G(\mathbf{x},t)\right) - H\left(G(\mathbf{x}_i,t)\right)\right)\right] \tag{26}$$

$$p^h(\mathbf{x},t) = \sum_i N_i(\mathbf{x}) \left[p_i(t) + b_i(t) \left(H\left(G(\mathbf{x},t)\right) - H\left(G(\mathbf{x}_i,t)\right)\right)\right]. \tag{27}$$

The jump conditions at the interface Γ are derived from mass and momentum conservation across the interface in the context of the hydrodynamic theory (see, e.g., [29]), known as the Rankine-Hugoniot relations. They may be written as follows:

$$[\![\mathbf{u}]\!] \cdot \mathbf{n} = -M[\![\rho^{-1}]\!] \quad \text{on } \Gamma, \tag{28}$$

$$[\![\mathbf{u}]\!] \cdot \mathbf{t}_1 = 0 \quad \text{on } \Gamma, \tag{29}$$

$$[\![\mathbf{u}]\!] \cdot \mathbf{t}_2 = 0 \quad \text{on } \Gamma, \tag{30}$$

$$[\![p]\!] = M^2[\![\rho^{-1}]\!] \quad \text{on } \Gamma. \tag{31}$$

The bracket operator $[\![x]\!] = x^{\mathrm{b}} - x^{\mathrm{u}}$ defines the jump in a quantity across the interface, $\mathbf{t}_1$ and $\mathbf{t}_2$ represent the tangential vectors at the interface, and M the mass flux across the

flame front: $M = \rho^{\mathrm{b}} \left(\mathbf{u}^{\mathrm{f}} - \mathbf{u}^{\mathrm{b}}\right) \cdot \mathbf{n} = \rho^{\mathrm{u}}(\mathbf{u}^{\mathrm{f}} - \mathbf{u}^{\mathrm{u}}) \cdot \mathbf{n}$. Various strategies exist for enforcing the jumps across the interface weakly.

Following the procedure described in section 3, the residual-based extended variational multiscale finite element formulation for the incompressible Navier-Stokes equations is obtained analogously to equations (15) and (16) using the corresponding density ρ and viscosity μ in the volume integrals over the subdomains Ω^b and Ω^u (see equation (12)). Of course, the rightmost terms in equations (15) and (18) and the last term in the second line in equation (16) do not exist in the present case. Depending on the strategy chosen to enforce the presented interface constraints weakly, additional surface integrals arise in the formulation. In [27], a Distributed Lagrange Multiplier (DLM) technique was used successfully for two-dimensional premixed combustion problems such as a Bunsen burner flame. Nitsche's method is applied in the context of reactive-diffusive scalar problems in [30] and for incompressible elasticity in [31] to account for Dirichlet and jump conditions in a weak sense. A different, stress-based, approach was proposed in [32] and adopted for the premixed combustion problem at hand. The resulting surface integrals are not presented in detail here. Integration over intersected elements and along the interface Γ is performed via integration cells obtained from a sub-tetrahedralization procedure as described in [27].

The residual-based variational formulation for the G-equation is derived in a straightforward manner applying the same steps as before and reads

$$\left(w^h, \tfrac{\partial G^h}{\partial t}\right) + \left(w^h, \mathbf{v}_f^h \cdot \nabla G^h\right) + \left(\mathbf{v}_f^h \cdot \nabla w^h, \tau_{\mathrm{G}} \mathcal{R}_{\mathrm{G}}^h\right) = 0, \tag{32}$$

with only an SUPG term included as in the energy conservation equation and the discrete residual of the G-equation given as

$$\mathcal{R}_{\mathrm{G}}^h = \frac{\partial G^h}{\partial t} + \mathbf{v}_f^h \cdot \nabla G^h. \tag{33}$$

Adopting (21) for the G-equation yields

$$\tau_{\mathrm{G}} = \frac{1}{\sqrt{\left(\frac{2}{\Delta t}\right)^2 + \mathbf{u}^h \cdot \mathbf{G}\mathbf{u}^h}}. \tag{34}$$

5 NUMERICAL EXAMPLES

In the following, a numerical example for turbulent variable-density flow at low Mach number, turbulent flow over a backward-facing step with heating, will be presented. More details on this example as well as further numerical examples for this problem type can be found in [21]. Numerical examples for premixed combustion using the extended method presented above are contained in [27].

Turbulent flow over a backward-facing step with heating is considered as a challenging numerical test case. The Reynolds number based on the step height, which is $h = 0.041$

m, and the mean inflow centerline velocity u_{1c} is 5580. The expansion ratio, that is, the ratio of the channel height downstream and upstream of the step, is 1.5, and a wall heat flux of $q_W = 2000$ W/m^2 is prescribed at the bottom wall behind the step. The geometry of the problem domain is depicted in Fig. 1. The problem configuration is similar to the one in [6], which is the only LES of variable-density flow at low Mach number in such a configuration so far, to the best of the authors' knowledge. Given the same expansion ratio, the Reynolds number in [6] was 5540, and thus almost identical to the present one. Further wall heat fluxes besides the one used here were investigated in [6]. LES data from [6] are denoted by "LES AP02" when used below.

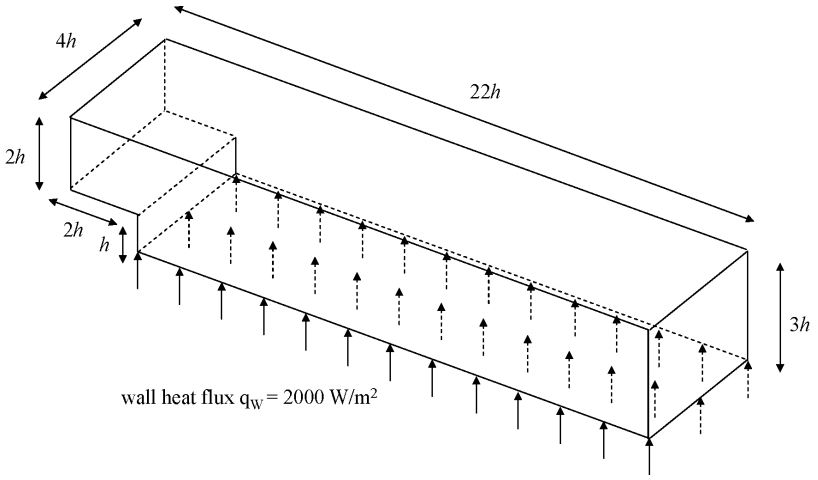

Figure 1: Geometry of problem domain for backward-facing step.

Snapshots of velocity and temperature distributions at the beginning of the statistical period are provided in Fig. 2; the hot spots at the heated bottom wall in the vicinity of the step wall are clearly observable. Velocity results at various locations behind the step (for the lower region of the problem domain) are depicted in Fig. 3. Besides the LES data from [6], (isothermal) experimental results from [33] are also included, which were used in [6] as reference results as well. This already indicates that the velocity results are to be expected close to respective isothermal results. The results in Fig. 3 confirm this observation. Differences between the three methodical combinations are hardly visible, and the reference results are sufficiently well matched. At the first five locations, the present results are even somewhat closer to the experimental results than the LES AP02 data. Further downstream, the LES AP02 results are very close to the present ones.

Fig. 4 shows the temperature results at various locations after the step, scaled by the reference temperature and only for the region close to the bottom wall. As can be seen, the temperature values undergo substantial variations within small distances from the bottom wall. At about 0.02 m above the bottom wall, the reference temperature is almost reached again, but at the bottom wall, a maximum overheating of about up to 300% of the reference temperature is observed. The LES AP02 results at locations $x_1 = h$

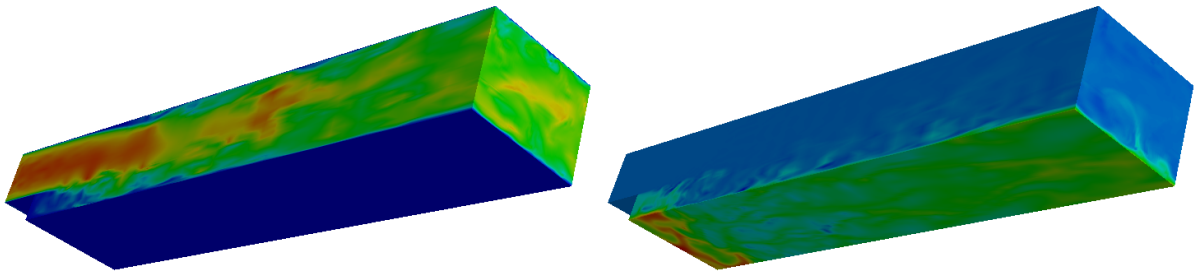

Figure 2: Snapshots of velocity and temperature distributions at the beginning of the statistical period, left: colored velocity magnitude distribution, right: colored temperature distribution (red color indicates high velocity/temperature, blue color low velocity/temperature).

and $x_1 = 3h$ are notably lower than the present ones and at locations $x_1 = 5h$, $x_1 = 7h$ and $x_1 = 9h$, they closely match. At the first location, $x_1 = h$, there is also a notable difference between the temperatures obtained with AVSSUP and the ones obtained with SUPSUP, SCRSUP as well as ALLSUP. Since there are no other reference results in this context, we would like to oppose our results against the LES AP02. In particular, our suspicion is that the profile yielded by AVSSUP might be close to the actual temperature distribution. A DNS would probably clarify the actual temperature distribution in this region.

6 CONCLUSIONS

An algebraic variational multiscale-multigrid method has been proposed for large-eddy simulation of turbulent variable-density flow at low Mach number as well as an extended approach towards premixed combustion. Scale-separating operators generated by level-transfer operators from plain aggregration algebraic multigrid methods enable the application of modeling terms to selected scale groups in a purely algebraic way. In the present context, this application of a modeling term is restricted to the smaller of the resolved problem scales. Following this purely algebraic strategy for scale separation means that no coarse discretization besides the basic one is required, in contrast to earlier approaches based on geometric multigrid methods. For the numerical example of turbulent flow past a backward-facing step with heating, a rather complex test problem, the results have been compared to other experimental and numerical results in literature. Promising results for two-dimensional premixed combustion problems using a Distributed Lagrange Multiplier (DLM) technique for enforcing interface conditions were achieved in [27]. The latter results have not been presented in the context of this article, and the reader is referred to the original publication for details.

7 ACKNOWLEDGEMENTS

The support of the first and second author via the Emmy Noether Program of the Deutsche Forschungsgemeinschaft (DFG) is gratefully acknowledged.

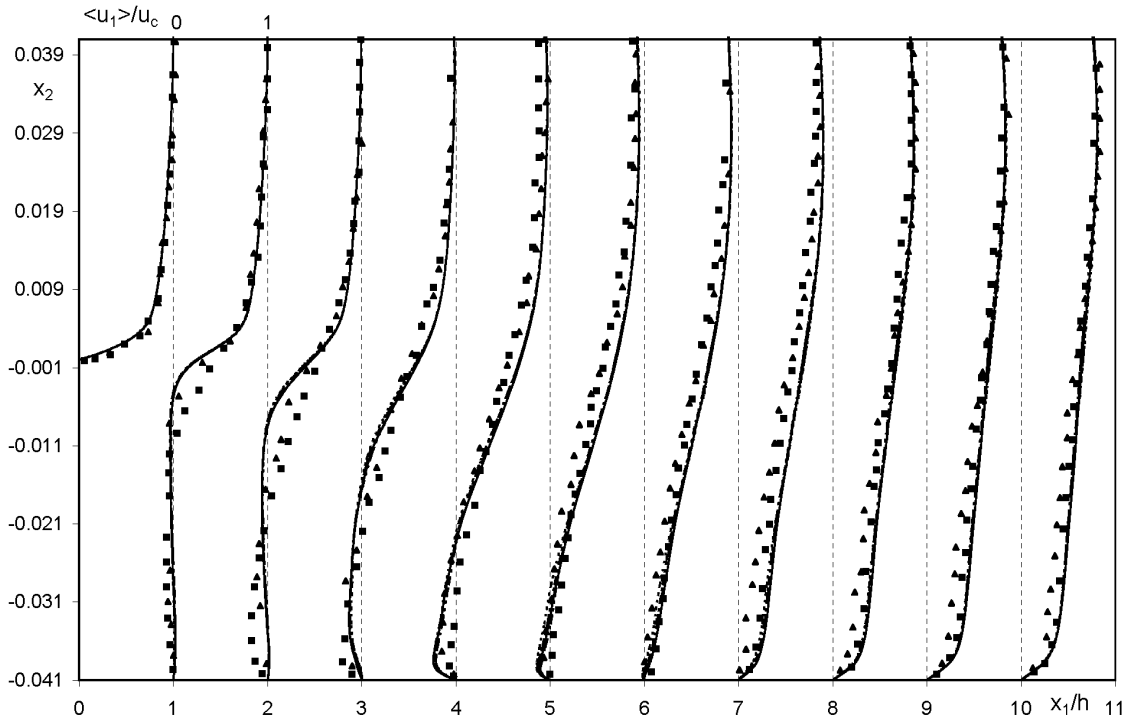

Figure 3: Velocity results for backward-facing step, solid lines: AVSSUP, dashed lines: SCRSUP, dotted-dashed lines: ALLSUP, double-dotted-dashed lines: SUPSUP, squares: LES AP02, triangles: EXP KM95.

REFERENCES

[1] P. Sagaut, Large eddy simulation for incompressible flows, third ed., Springer-Verlag, Berlin, 2006.

[2] E. Garnier, N. Adams, P. Sagaut, Large eddy simulation for compressible flows, Scientific Computation, Springer, 2009.

[3] A. Majda, J. Sethian, The derivation and numerical solution of the equations for zero Mach number combustion, Combust. Sci. Tech. 42 (1985) 185–205.

[4] N. Peters, Turbulent combustion, Cambridge University Press, Cambridge, 2000.

[5] C. Pierce, P. Moin, Progress-variable approach for large eddy simulation of turbulent combustion, Report TF80, Flow Physics and Computation Division, Department of Mechanical Engineering, Stanford University, 2001.

[6] R.V.R. Avancha, R.H. Pletcher, Large eddy simulation of the turbulent flow past a backward–facing step with heat transfer and property variations, Int. J. Heat Fluid Flow 23 (2002) 601–614.

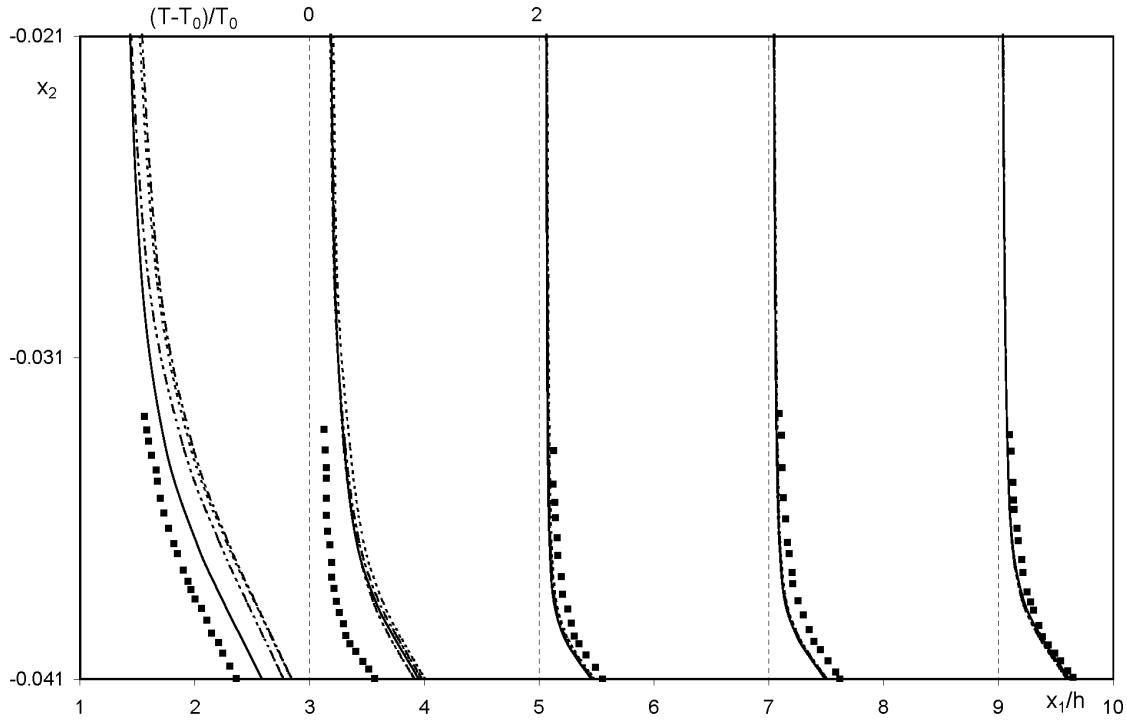

Figure 4: Temperature results for backward-facing step, solid lines: AVSSUP, dashed lines: SCRSUP, dotted-dashed lines: ALLSUP, double-dotted-dashed lines: SUPSUP, squares: LES AP02.

[7] B. Lessani, M.V. Paplexandris, Time-accurate calculation of variable density flows with strong temperature gradients and combustion, J. Comput. Phys. 212 (2006) 218-246.

[8] O. Desjardins, G. Blanquart, G. Balarac, H. Pitsch, High order conservative finite difference scheme for variable density low Mach number turbulent flows, J. Comput. Phys. 227 (2008) 7125–7159.

[9] V. Heuveline, On higher-order mixed FEM for low Mach number flows: Applications to a natural convection benchmark problem, Int. J. Numer. Methods Fluids 41 (2003) 1339-1356.

[10] M.J. Martinez, D.K. Gartling, A finite element method for low-speed compressible flows, Comput. Methods Appl. Mech. Engrg. 193 (2004) 1959–1979.

[11] J. Principe, R. Codina, A stabilized finite element approximation of low speed thermally coupled flows, Int. J. Num. Meth. Heat Fluid Flow 18 (2008) 835–867.

[12] G. Hauke, L. Valiño, Computing reactive flows with a field Monte Carlo formulation and multi-scale methods, Comput. Methods Appl. Mech. Engrg. 193 (2004) 1455-1470.

[13] J.N. Shadid, R.S. Tuminaro, K.D. Devine, G.L. Hennigan, P.T. Lin, Performance of fully coupled domain decomposition preconditioners for finite element transport/reaction simulations, J. Comput. Phys. 205 (2005) 24-47.

[14] M. Braack, T. Richter, Stabilized finite elements for 3-D reactive flows, Int. J. Numer. Methods Fluids 51 (2006) 981-999.

[15] V. Gravemeier, M.W. Gee, W.A. Wall, An algebraic variational multiscale-multigrid method based on plain aggregation for convection-diffusion problems, Comput. Methods Appl. Mech. Engrg. 198 (2009) 3821–3835.

[16] V. Gravemeier, M.W. Gee, M. Kronbichler, W.A. Wall, An algebraic variational multiscale-multigrid method for large eddy simulation of turbulent flow, Comput. Methods Appl. Mech. Engrg. 199 (2010) 853–864.

[17] T.J.R. Hughes, L. Mazzei, K.E. Jansen, Large eddy simulation and the variational multiscale method, Comput. Visual. Sci. 3 (2000) 47–59.

[18] S.S. Collis, Monitoring unresolved scales in multiscale turbulence modeling, Phys. Fluids 13 (2001) 1800-1806.

[19] V. Gravemeier, The variational multiscale method for laminar and turbulent flow, Arch. Comput. Meth. Engng. 13 (2006) 249–324.

[20] P.T. Lin, M. Sala, J.N. Shadid, R.S. Tuminaro, Performance of fully coupled algebraic multilevel domain decomposition preconditioners for incompressible flow and transport, Int. J. Numer. Meth. Engrg. 67 (2006) 208–225.

[21] V. Gravemeier, W.A. Wall, An algebraic variational multiscale-multigrid method for large-eddy simulation of turbulent variable-density flow at low Mach number, Preprint, submitted for publication in J. Comput. Phys., 2009.

[22] F.A. Williams, Turbulent combustion, in: J. Buckmaster (Ed.), The Mathematics of Combustion, SIAM, Philadelphia, 1985, pp. 97-131.

[23] S. Osher, J.A. Sethian, Fronts propagating with curvature-dependent speed: Algorithms based on Hamilton-Jacobi formulations, J. Comput. Phys. 79 (1988) 12–49.

[24] H. Pitsch, L. Duchamp de Lageneste, Large-eddy simulation of premixed turbulent combustion using a level-set approach, Proc. Combust. Inst. 29 (2002) 2001–2008.

[25] N. Moës, J. Dolbow, T. Belytschko, A finite element method for crack growth without remeshing, Int. J. Numer. Methods Engng. 46 (1999) 131–150.

[26] J. Chessa, T. Belytschko, An enriched finite element method and level sets for axisymmetric two-phase flow with surface tension, Int. J. Numer. Meth. Engng. 58 (2003) 2041–2064.

[27] F. van der Bos, V. Gravemeier, Numerical simulation of premixed combustion using an enriched finite element method, J. Comput. Phys. 228 (2009) 3605–3624.

[28] F. Losasso, R. Fedkiw, S. Osher, Spatially adaptive techniques for level set methods and incompressible flow, Comput. Fluids 35 (2006) 995–1010.

[29] M. Matalon, B.J. Matkowsky, Flames as gasdynamic discontinuities, J. Fluid Mech. 124 (1982) 239–259.

[30] J. Dolbow, I. Harari, An efficient finite element method for embedded interface problems, Int. J. Numer. Meth. Engng. 78 (2009) 229–252.

[31] R. Becker, E. Burman, P. Hansbo, A Nitsche extended finite element method for incompressible elasticity with discontinuous modulus of elasticity, Comput. Methods Appl. Mech. Engrg. 198 (2009) 3352–3360.

[32] A. Gerstenberger, W.A. Wall, An embedded Dirichlet formulation for 3D continua, Int. J. Numer. Meth. Engng. 82 (2010) 537–563.

[33] N. Kasagi, A. Matsunaga, Three-dimensional particle-tracking velocimetry measurement of turbulence statistics and energy budget in a backward-facing step flow, Int. J. Heat Fluid Flow 16 (1995) 477–485.